Article

Not peer-reviewed version

Correlating the $0\nu\beta\beta$-Decay Amplitudes of ^{136}Xe with the Ordinary Muon Capture (OMC) Rates of ^{136}Ba

Aagrah Agnihotri * , Vikas Kumar , Jouni Suhonen

Posted Date: 21 March 2025

doi: 10.20944/preprints202503.1465.v1

Keywords: double beta decay of Xe-136; nuclear matrix elements; muon capture on Ba-136; muon-capture rates

Article

Correlating the $0\nu\beta\beta$-Decay Amplitudes of ^{136}Xe with the Ordinary Muon Capture (OMC) Rates of ^{136}Ba

Aagrah Agnihotri [1,2,*], Vikas Kumar [1,3] and Jouni Suhonen [1,2]

1 University of Jyväskylä, Department of Physics, P.O. Box 35 (YFL), 40014 Jyväskylä, Finland;
2 International Centre for Advanced Training and Research in Physics (CIFRA), P.O. Box MG12, 077125, Bucharest-Măgurele, Romania
3 Banaras Hindu University, Varanasi, Uttar Pradesh, 221005, India
* Correspondence: aagrah.a.agnihotri@jyu.fi

Abstract: The potential correlation between the ordinary muon capture (OMC) on ^{136}Ba and $0\nu\beta\beta$ decay of ^{136}Xe is explored. For this we have computed $0\nu\beta\beta$-decay amplitudes for intermediate states in ^{136}Cs below 1 MeV of excitation and for angular-momentum values $J \leq 5$ by using the proton-neutron quasiparticle random-phase approximation (pnQRPA) and nuclear shell model (NSM). We compare these amplitudes with the corresponding OMC rates, computed in a previous Universe article (Universe **2023**, 9, 270) for the same energy and angular-momentum ranges. The obtained results suggest that an extension of the present analysis to a wider energy and angular-momentum region could be highly beneficial for probing the $0\nu\beta\beta$-decay nuclear matrix elements using experimental data on OMC rates to intermediate states of $0\nu\beta\beta$ decays.

Keywords: double beta decay of Xe-136; nuclear matrix elements; muon capture on Ba-136; muon-capture rates

---

1. Introduction

The theoretical study of the hypothesized rare neutrinoless double beta ($0\nu\beta\beta$) decay is a challenging, yet among the most promising avenues of searches of physics beyond the standard model [1–5]. The complexity in the study of $0\nu\beta\beta$ decay stems from the involvement of nuclear-structure effects/correlations from low to high momentum-exchange scales ($q \leq 100 - 200$ MeV) and nuclear states of high energy and/or multipolarity (J^π). Experimental nuclear-structure data at medium and high momentum scales is seldom available and is almost entirely uncharted territory, making it difficult for nuclear models and hence the computed $0\nu\beta\beta$ nuclear matrix elements (NMEs) to be improved upon being tuned to such data. Given that $0\nu\beta\beta$ decay has not been measured, accurate nuclear modeling of this process for various $0\nu\beta\beta$-decay candidates is essential for determining the sensitivity of experiments designed to detect this rare decay [6]. There are significant discrepancies in the $0\nu\beta\beta$-decay NMEs computed in various nuclear-model frameworks [1], and imperfect nuclear-structure calculations demand the use of an effective value of the axial vector coupling (g_A^{eff}) [5–8]. Discrepancies in $0\nu\beta\beta$-decay NMEs across nuclear models and uncertainty in the value of g_A^{eff} propagate in the 2$^{\text{nd}}$ and 4$^{\text{th}}$ power, respectively, to the computed/predicted half-lives.

Ordinary muon capture (OMC) is a seemingly miraculous process in that it is the only known practical way to systematically investigate the nuclear structure experimentally at momentum scales relevant to the physics of $0\nu\beta\beta$ decay [9–12]. OMC can also populate all the nuclear states that are intermediate states of the odd-odd nucleus, via which the $0\nu\beta\beta$ decay proceeds [9–12]. This means that OMC can and is used to access decay amplitudes of one leg, involving either the daughter or the mother nucleus of the "two-step" rare transition, depending on whether $0\nu\beta\beta$ is of β^- or β^+/EC type, respectively [9–13]. Involvement of common decay amplitudes in this way for the computed OMC NMEs/rates and $0\nu\beta\beta$-decay NMEs leads us to look for connections between the two. Towards both

Preprints.org (www.preprints.org) | NOT PEER-REVIEWED | Posted: 21 March 2025 doi:10.20944/preprints202503.1465.v1

ends of computing more accurate $0\nu\beta\beta$-decay NMEs and determination of g_A^{eff}, the OMC process is a gift from nature as it can help address both of these goals. The study of OMC is the best-known way to test the fitness of nuclear models and improve their accuracy, by closely tuning them to experimental data for computing physically relevant OMC NMEs. Tuning the nuclear models this way makes them optimized to compute $0\nu\beta\beta$-decay amplitudes and ultimately NMEs due to similar nuclear and weak-interaction contributions involved in the two processes [10–12,14]. As an example, OMC can give us access to the value of the particle-particle interaction parameter (g_{pp}) in the pnQRPA (proton-neutron quasiparticle random-phase approximation) framework [10–12], and g_A^{eff} and/or the effective value of the pseudoscalar coupling (g_P) [15–29] at momentum scales relevant for $0\nu\beta\beta$ decay.

Only in the recent past, major experimental efforts have been made to leverage OMC to illuminate further the mystery of $0\nu\beta\beta$ decay, by measuring (partial) OMC rates as being done in present state-of-the-art experiments such as the MONUMENT experiment [30]. Such experiments will make available invaluable experimental constraints for grounding the theoretical modeling of OMC processes, and offering a tangible map for the improvement of nuclear models, leading the way to more accurate computed OMC/$0\nu\beta\beta$-decay NMEs.

The connection of having common decay amplitudes in the computed NMEs of the two processes prompted the search for the potential correlations and trends between $0\nu\beta\beta$-decay NMEs and OMC rates/NMEs as presented in References [10–12,31]. Such connections can be used to determine the accuracy of the computed $0\nu\beta\beta$-decay NMEs. In Reference [31], average OMC NMEs and $0\nu\beta\beta$-decay NMEs for key $0\nu\beta\beta$-decay candidates including ^{136}Xe (the focus of this work) were compared in the framework of pnQRPA, and systematic correspondences were observed between the two. The NMEs were compared in order to minimize the kinematic and phase-space effects in the anticipated correlations. Given the trends observed in Reference [31], we anticipate seeing this correspondence map to correspondences between OMC rates and $0\nu\beta\beta$-decay NMEs. Evidence for such a connection is foreshadowed from trends between OMC rates and $2\nu\beta\beta$-decay NMEs as presented in References [10–12]. Correlations between OMC rates and $0\nu\beta\beta$-decay NMEs are of high interest as this can be a direct bridge between experimental OMC rates and theoretical $0\nu\beta\beta$-decay NMEs.

The focus of this work is to further elucidate this bridge in the context of $0\nu\beta\beta$ decaying ^{136}Xe, using for the first time the pnQRPA and nuclear shell model (NSM) together in OMC and non-closure $0\nu\beta\beta$ formalisms. We compute the $0\nu\beta\beta$-decay amplitudes in the above frameworks and compare them with results obtained for the OMC rates of ^{136}Ba, as presented in Reference [32], using the same nuclear models. In using different nuclear models, one can see if the potential correlations are model-independent and follow the similarities and differences in the trends that emerge.

2. Theory

2.1. Nuclear-Model Calculations

In the present work we adopt the nuclear shell model (NSM) and the proton-neutron quasiparticle random-phase approximation (pnQRPA) [33] as the basic nuclear-model frameworks. We compute the wave functions of the states of the odd-odd nucleus ^{136}Cs by using these models in order to access the $0\nu\beta\beta$-decay amplitudes in a non-closure approach and compare them with the corresponding OMC rates computed in Reference [32]. In both the OMC and $0\nu\beta\beta$ calculations we use the phenomenological NSM (**sm-phen**) and pnQRPA (**qrpa-phen**) approach, with the relevant parameters defined in Table 1 of Reference [32]. As in [32], the decay amplitudes are computed for states with excitation energy ≤ 1 MeV, an energy range relevant to present-day MONUMENT experiment [30].

2.2. Ordinary Muon Capture (OMC)

The OMC is a well-studied nuclear process, both experimentally and theoretically [9]. In this work we compare our calculated $0\nu\beta\beta$-decay amplitudes with the OMC rates of Reference [32]. The OMC

 doi:10.20944/preprints202503.1465.v1

formalism of Reference [32] is an extended Morita-Fujii formalism described in detail in [34,35]. Lately, the use of realistic muon wave functions has been implemented [36], and up-to-date computations for OMC rates of ^{136}Ba have been presented in Reference [32]. We refer readers to these results as we use them for the purposes of this work. For completeness, we present here some key relations for computing the OMC rates, where OMC of ^{136}Ba proceeds as:

$$\mu^- + ^{136}\mathrm{Ba}(0^+_{g.s.}) \rightarrow \nu_\mu + ^{136}\mathrm{Cs}(J^\pi_f), \tag{1}$$

where a negative muon (μ^-) is captured by the ground state of ^{136}Ba, leading to final states J^π_f in ^{136}Cs. At the same time, a muon neutrino (ν_μ) is emitted. The general expression of the OMC rate is given as:

$$W = 2P(2J_f + 1)\left(1 - \frac{q}{m_\mu + AM}\right)q^2, \tag{2}$$

where the momentum exchange q is expressed as

$$q = (m_\mu - W_0)\left(1 - \frac{m_\mu}{2(m_\mu + AM)}\right). \tag{3}$$

Here, J_f is the final-state spin-parity, M is the average nucleon mass, A is the nuclear mass number, and m_μ (m_e) is the rest mass of the muon (electron). The threshold energy is given by

$$W_0 = M_f - M_i + m_e + E_X, \tag{4}$$

where M_i and M_f are the masses of the initial and final nuclei, and E_X is the excitation energy of the final nuclear state, in our case of ^{136}Cs. The rate function P contains the NMEs, phase-space factors, and combinations of weak couplings g_A (axial-vector), g_P (induced pseudoscalar), and $g_M = 1 + \mu_p - \mu_n$ (induced weak-magnetism), with μ_p and μ_n being the anomalous magnetic moments of the proton and neutron, respectively.

2.3. $0\nu\beta\beta$ Decay

The computational scheme used here is presented in detail in Reference [37]. We present here key relations. Assuming light Majorana neutrino exchange [4,37], the inverse half-life can be written as

$$\left[t^{(0\nu)}_{1/2}(0^+_i \rightarrow 0^+_f)\right]^{-1} = g_A^4 G_{0\nu}\left|M^{(0\nu)}\right|^2 |\langle m_\nu \rangle|^2, \tag{5}$$

where $G_{0\nu}$ is the phase-space factor for the final-state leptons, g_A is the axial vector coupling constant, $\langle m_\nu \rangle$ is the effective neutrino mass, and $M^{(0\nu)}$ is the nuclear matrix element (NME). The $M^{(0\nu)}$ NME can be decomposed as:

$$M^{(0\nu)} = M^{(0\nu)}_{\mathrm{GT}} - \left(\frac{g_V}{g_A}\right)^2 M^{(0\nu)}_{\mathrm{F}} + M^{(0\nu)}_{\mathrm{T}}, \tag{6}$$

where $M^{(0\nu)}_{\mathrm{GT}}$, $M^{(0\nu)}_{\mathrm{F}}$, and $M^{(0\nu)}_{\mathrm{T}}$ are the Gamow-Teller, Fermi, and Tensor components of the NME, respectively, and g_V is the vector coupling constant. Contribution from various multipoles constituting all the intermediate transitions is given as :

$$M^{(0\nu)}_K = \sum_{J^\pi} M^{(0\nu)}_K(J^\pi), \tag{7}$$

where $K = \mathrm{GT}, \mathrm{F}, \mathrm{T}$, and $M^{(0\nu)}_K(J^\pi)$ are the contributions from all the states i of an the intermediate multipole J^π. Each multipole contribution is, in turn, decomposed in terms of the two-particle transition matrix elements and one-body transition densities. In the pnQRPA calculations the two-particle transition matrix element reads

$$M_K^{(0\nu)}(J^\pi) = \sum_{k_1,k_2,J'} \sum_{pp',nn'} (-1)^{j_n+j_{p'}+J+J'} \sqrt{2J'+1} \begin{Bmatrix} j_p & j_n & J \\ j_{n'} & j_{p'} & J' \end{Bmatrix} \times$$
$$(pp' : J'|O_K|nn' : J') \left(0_f^+||[c_{p'}^\dagger \tilde{c}_n]_J||J_{k_1}^\pi\right) \langle J_{k_1}^\pi | J_{k_2}^\pi \rangle \left(J_{k_2}^\pi||[c_p^\dagger \tilde{c}_n]_J||0_i^+\right), \quad (8)$$

where k_1, k_2 label the pnQRPA solutions for a given multipole J^π, starting from the final (k_1) and initial (k_2) nuclei, and p, p', n, n' denote the proton and neutron single-particle quantum numbers. The operator O_K contains the neutrino potentials, the characteristic two-particle operators for the different K components, and short-range correlation effects. The quantities $\left(0_f^+||[c_{p'}^\dagger \tilde{c}_n]_J||J_{k_1}^\pi\right)$ and $\left(J_{k_2}^\pi||[c_p^\dagger \tilde{c}_n]_J||0_i^+\right)$ are the corresponding decay amplitudes and $\langle J_{k_1}^\pi | J_{k_2}^\pi \rangle$ is an overlap factor connecting the two branches of pnQRPA solutions for the ^{136}Cs wave functions.

In the NSM calculations we use one unique set of states in ^{136}Cs so that the sum over k_1, k_2 in Equation (8) is replaced by a sum over a single state number k and the overlap factor is not needed.

3. Results and Discussion

In order to compare the OMC rates and $0\nu\beta\beta$-decay amplitudes for J_k^π states in a meaningful way, we consider the following physical assumptions: both quantities depend on the energy ($E_k(J_k^\pi)$), multipolarity (J^π), and nuclear-structure content of the J_k^π (virtual) states being populated in the process. In the case of OMC rates, phase-space factors contribute directly to OMC rates. For $0\nu\beta\beta$-decay NMEs, the dependence of neutrino potentials on energy, affects the concerned decay amplitudes. For our analysis, we can assume the energy dependence to be a constant for all the states since their energy is ≤ 1 MeV. Therefore, our analysis simplifies, and we attribute the observed trends in OMC rates and $0\nu\beta\beta$-decay amplitudes to multipolarity (J^π) and nuclear-structure content of J_k^π states. We see effects of such dependencies in the computed $0\nu\beta\beta$-decay amplitudes presented in Tables 1 and 2 for the aforementioned computational scheme in Section 2.1.

Computed OMC rates for individual J_k^π states can be found in Reference [32]. In order to smooth out the variations of the OMC rates and $0\nu\beta\beta$-decay amplitudes from one individual J^π state to the other, we study the combined contribution to a given multipole J^π, an effective strategy already implemented in Reference [31]. Another important consideration is that given that the nuclear-structure calculations are not perfect, we only consider the trends within the same nuclear model. So for the purposes of this paper, we look at trends in pnQRPA (**qrpa-phen**) and NSM (**sm-phen**) results independently. In Table 3, the cumulative OMC rates OMC(J^π) and amplitude contributions to $M^{(0\nu)}(J^\pi)$ for multipole J^π are given, and also plotted in Figures 1 and 2.

 doi:10.20944/preprints202503.1465.v1

Table 1. Phenomenological pnQRPA-computed $0\nu\beta\beta$-decay amplitudes of the NMEs of Equation (6). The amplitudes are given in units of 10^{-3}.

J^π	$E_{\rm exc}$ [keV]	$M_{\rm F}$	$M_{\rm GT}$	$M_{\rm T}$	$M^{(0\nu)}$
5_1^+	0	0	-0.18	0.040	-0.14
3_1^+	102	0	-0.28	0.037	-0.24
2_1^+	120	0.20	-0.13	-0.034	-0.46
4_1^+	154	0.07	-0.02	-0.006	-0.13
1_1^+	193	0	-1.61	0.021	-1.59
4_2^+	203	4.96	-0.32	-0.13	-7.65
3_2^+	264	0	-51.6	16.3	-35.2
3_3^+	281	0	-10.1	0.88	-9.20
3_4^+	338	0	-9.46	-3.27	-12.7
2_2^+	367	0.01	-0.16	-0.0041	-0.22
3_1^-	458	0.02	-0.16	-0.0060	-0.25
4_3^+	494	-0.007	-0.24	-0.089	-0.32
5_1^-	515	0.03	-0.11	-0.050	-0.21
4_1^-	558	0	-0.42	0.068	-0.35
2_3^+	561	5.29	-24.5	-8.22	-40.4
5_2^-	637	0.07	-0.01	-0.004	-0.12
4_2^-	695	0	-0.24	0.084	-0.16
2_1^-	704	0	-0.49	0.097	-0.40
3_2^-	926	0.23	-0.02	-0.008	-0.36

Table 2. Phenomenological NSM-computed $0\nu\beta\beta$-decay amplitudes of the NMEs of Equation (6). The amplitudes are given in units of 10^{-3}.

J^π	$E_{\rm exc}$ [keV]	$M_{\rm F}$	$M_{\rm GT}$	$M_{\rm T}$	$M^{(0\nu)}$
5_1^+	0	0	-4.355	1.411	-2.944
3_1^+	23	0	-5.695	1.445	-4.250
4_1^+	39	1.230	-0.153	-0.058	-1.633
2_1^+	83	6.993	-5.160	-1.433	-14.677
3_2^+	181	0	-2.269	-0.555	-2.824
2_2^+	224	0.894	-4.481	-1.748	-7.262
3_3^+	244	0	-1.647	-0.059	-1.706
4_2^+	323	1.989	-2.575	-1.019	-5.895
4_3^+	498	2.582	-3.525	-1.578	-8.088
3_4^+	517	0	6.540	-0.289	6.251
5_1^-	522	0.723	-2.483	-1.048	-4.366
3_1^-	545	0.379	-4.893	-1.701	-7.033
1_1^+	545	0	33.820	-1.602	32.218
4_1^-	547	0	5.565	0.589	6.154
2_3^+	615	-1.426	2.804	0.780	5.232
5_2^-	670	1.313	-0.511	-0.210	-2.239
1_2^+	752	0	6.066	-0.064	6.003
4_2^-	760	0	-1.281	0.309	-0.972
2_4^+	803	0.290	-0.889	-0.251	-1.475
4_4^+	885	0.082	-0.108	-0.044	-0.248
2_1^-	1016	0	-44.144	0.371	-43.772

doi:10.20944/preprints202503.1465.v1

Table 3. Cumulative $0\nu\beta\beta$-decay amplitudes $M^{(0\nu)}(J^\pi)$ and OMC rates OMC(J^π) for multipoles $J^\pi \leq 5$. OMC rates and the decay amplitudes are given units of 10^3 1/s and 10^{-3}, respectively.

	qrpa-phen		**sm-phen**	
J^π	$M^{(0\nu)}(J^\pi)$	OMC(J^π)	$M^{(0\nu)}(J^\pi)$	OMC(J^π)
5^+	-0.14	0.50	-2.944	0.0
4^+	-8.10	20.4	-15.864	9.8
3^+	-57.4	87.8	-2.529	29.9
2^+	-41.0	201.1	-18.182	34.9
1^+	-1.59	206.9	38.221	5.2
5^-	-0.33	0.80	-6.605	0.6
4^-	-0.52	21.2	5.182	15.0
3^-	-0.61	38.7	-7.033	9.7
2^-	-0.40	14.2	-43.772	44.4

In the figures positive and negative multipoles are plotted separately for clarity, and the quantities are scaled appropriately for optimal comparison. As seen from the plots in Figures 1 and 2, regular variations between the quantities are observed. The variation of OMC rates (J^π) and $M^{(0\nu)}(J^\pi)$ look roughly "mirror reflection" of each other, both in the context of pnQRPA, and NSM. Further conclusions cannot be made given the limited number of states and multipolarity, but the results look promising, giving impetus to a larger-scale study involving a larger set of states for each multipolarity, and covering a larger range of multipolarities, possibly to the Gamow-Teller giant resonance region in the case of the pnQRPA.

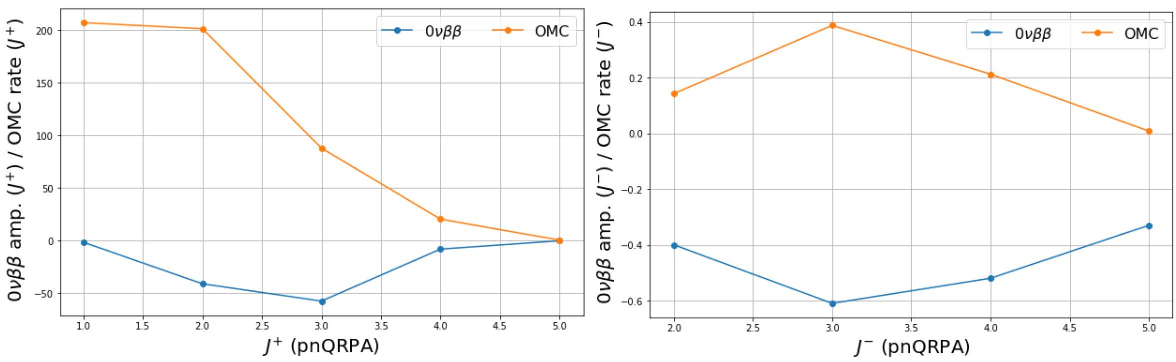

(a) $M^{(0\nu)}(J^+)$ (in units of 10^{-3}) and OMC(J^+) (in units of 10^3 1/s) vs J^+

(b) $M^{(0\nu)}(J^-)$ (in units of 10^{-3}) and OMC(J^-) (in units of 10^5 1/s) vs J^-

Figure 1. Cumulative $0\nu\beta\beta$-decay amplitudes and OMC rates for J^π states computed using pnQRPA (**qrpa-phen**). The decay amplitudes and OMC rates have been scaled appropriately for optimal comparison.

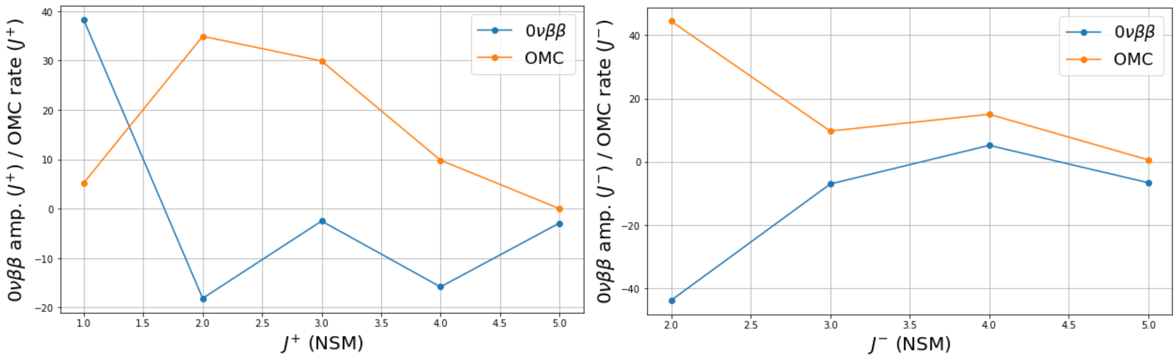

(a) $M^{(0\nu)}(J^+)$ (in units of 10^{-3}) and OMC(J^+) (in units of 10^3 1/s) vs J^+

(b) $M^{(0\nu)}(J^-)$ (in units of 10^{-3}) and OMC(J^-) (in units of 10^3 1/s) vs J^-

Figure 2. Cumulative $0\nu\beta\beta$-decay amplitudes and OMC rates for J^π states computed using NSM (**sm-phen**). The decay amplitudes and OMC rates have been scaled appropriately for optimal comparison.

4. Conclusions

Correlations between the ordinary muon capture (OMC) on ^{136}Ba and $0\nu\beta\beta$ decay of ^{136}Xe were searched for using $0\nu\beta\beta$-decay intermediate states in ^{136}Cs below 1 MeV of excitation and for angular-momentum values $J \leq 5$. We computed $0\nu\beta\beta$-decay amplitudes through these intermediate states by using the proton-neutron quasiparticle random-phase approximation (pnQRPA) and nuclear shell model (NSM). Comparison with a corresponding earlier OMC calculation suggests that there are "mirror type of" correlations between the $0\nu\beta\beta$-decay amplitudes and the OMC rates. These correlations suggest that an extension of the present analysis to a wider energy and angular-momentum region could lead to a practical way to probe the $0\nu\beta\beta$-decay nuclear matrix elements using experimental data on OMC rates to intermediate states of $0\nu\beta\beta$ decays.

Author Contributions: Calculation of $0\nu\beta\beta$-decay amplitudes using NSM, figures, primary analyses, writing the first draft, A.A.; NSM calculations, preparation of $0\nu\beta\beta$ calculation input files for NSM (used by A.A.), V.K.; original idea of the project, computing $0\nu\beta\beta$-decay amplitudes using pnQRPA, coordination and supervision of the computations and analyses, finalizing the text of the draft, J.S.

Funding: A.A. and J.S. acknowledge support from project PNRR-I8/C9-CF264, Contract No. 760100/23.5.2023 of the Romanian Ministry of Research, Innovation and Digitization (the NEPTUN project). V.K. acknowledges financial support from 'GEFP' IoE BHU fellowship (R/Dev/D/IoE/2024-25/GEFP/76559), and SERB Project (File No. EEQ/2023/000157), Govt. of India.

Data Availability Statement: Not applicable

Acknowledgments: We acknowledge grants of computer capacity from the Finnish Grid and Cloud Infrastructure (persistent identifier urn:nbn:fi:research-infras-2016072533), the support by CSC – IT Center for Science, Finland, for the generous computational resources.

Conflicts of Interest: The authors declare no conflicts of interest.

References

1. Agostini, M.; Benato, G.; Detwiler, J.A.; Menéndez, J.; Vissani, F. Toward the discovery of matter creation with neutrinoless $\beta\beta$ decay. *Rev. Mod. Phys.* **2023**, *95*, 025002.
2. Blaum, K.; Eliseev, S.; Danevich, F.A.; Tretyak, V.I.; Kovalenko, S.; Krivoruchenko, M.I.; Novikov, Y.N.; Suhonen, J. Neutrinoless double-electron capture. *Rev. Mod. Phys.* **2020**, *92*, 045007.
3. Engel, J.; Menéndez, J. Status and future of nuclear matrix elements for neutrinoless double-beta decay: a review. *Reports on Progress in Physics* **2017**, *80*, 046301. https://doi.org/10.1088/1361-6633/aa5bc5.
4. Suhonen, J.; Civitarese, O. Weak-interaction and nuclear-structure aspects of nuclear double beta decay. *Physics Reports* **1998**, *300*, 123–214. https://doi.org/https://doi.org/10.1016/S0370-1573(97)00087-2.

5. Ejiri, H.; Suhonen, J.; Zuber, K. Neutrino–nuclear responses for astro-neutrinos, single beta decays and double beta decays. *Physics Reports* **2019**, *797*, 1.
6. Suhonen, J. Impact of the quenching of g_A on the sensitivity of $0\nu\beta\beta$ experiments. *Phys. Rev. C* **2017**, *96*, 055501.
7. Suhonen, J.T. Value of the Axial-Vector Coupling Strength in β and $\beta\beta$ Decays: A Review. *Frontiers in Physics* **2017**, *5*, 55.
8. Suhonen, J.; Kostensalo, J. Double β Decay and the Axial Strength. *Frontiers in Physics* **2019**, *7*, 29.
9. Measday, D. The nuclear physics of muon capture. *Physics Reports* **2001**, *354*, 243–409. https://doi.org/https://doi.org/10.1016/S0370-1573(01)00012-6.
10. Kortelainen, M.; Suhonen, J. Ordinary muon capture as a probe of virtual transitions of $\beta\beta$ decay. *Europhysics Letters* **2002**, *58*, 666. https://doi.org/10.1209/epl/i2002-00401-5.
11. Kortelainen, M.; Suhonen, J. Microscopic study of muon-capture transitions in nuclei involved in double-beta-decay processes. *Nuclear Physics A* **2003**, *713*, 501–521. https://doi.org/https://doi.org/10.1016/S0375-9474(02)01303-9.
12. Kortelainen, M.; Suhonen, J. Nuclear muon capture as a powerful probe of double-beta decays in light nuclei. *Journal of Physics G: Nuclear and Particle Physics* **2004**, *30*, 2003. https://doi.org/10.1088/0954-3899/30/12/017.
13. Jokiniemi, L.; Suhonen, J.; Kotila, J. Comparative analysis of nuclear matrix elements of $0\nu\beta^+\beta^+$ decay and muon capture in ^{106}Cd. *Frontiers in Physics* **2021**, *9*, 652536.
14. Šimkovic, F.; Pantis, G.; Vergados, J.D.; Faessler, A. Additional nucleon current contributions to neutrinoless double β decay. *Phys. Rev. C* **1999**, *60*, 055502. https://doi.org/10.1103/PhysRevC.60.055502.
15. Kolbe, E.; Langanke, K.; Vogel, P. Muon capture, continuum random phase approximation, and in-medium renormalization of the axial-vector coupling constant. *Phys. Rev. C* **1994**, *50*, 2576–2581. https://doi.org/10.1103/PhysRevC.50.2576.
16. Johnson, B.L.; Gorringe, T.P.; Armstrong, D.S.; Bauer, J.; Hasinoff, M.D.; Kovash, M.A.; Measday, D.F.; Moftah, B.A.; Porter, R.; Wright, D.H. Observables in muon capture on ^{23}Na and the effective weak couplings $\tilde{g}_a$ and $\tilde{g}_p$. *Phys. Rev. C* **1996**, *54*, 2714–2731. https://doi.org/10.1103/PhysRevC.54.2714.
17. Gorringe, T.P.; Armstrong, D.S.; Arole, S.; Boleman, M.; Gete, E.; Kuzmin, V.; Moftah, B.A.; Sedlar, R.; Stocki, T.J.; Tetereva, T. Measurement of partial muon capture rates in $1s-0d$ shell nuclei. *Phys. Rev. C* **1999**, *60*, 055501. https://doi.org/10.1103/PhysRevC.60.055501.
18. Siiskonen, T.; Suhonen, J.; Hjorth-Jensen, M. Shell-model effective operators for muon capture in ^{20}Ne. *Journal of Physics G: Nuclear and Particle Physics* **1999**, *25*, L55. https://doi.org/10.1088/0954-3899/25/8/102.
19. Siiskonen, T.; Hjorth-Jensen, M.; Suhonen, J. Renormalization of the weak hadronic current in the nuclear medium. *Phys. Rev. C* **2001**, *63*, 055501. https://doi.org/10.1103/PhysRevC.63.055501.
20. Auerbach, N.; Brown, B.A. Weak interaction rates involving ^{12}C, ^{14}N, and ^{16}O. *Phys. Rev. C* **2002**, *65*, 024322. https://doi.org/10.1103/PhysRevC.65.024322.
21. Gorringe, T.P.; Johnson, B.L.; Armstrong, D.S.; Bauer, J.; Kovash, M.A.; Hasinoff, M.D.; Measday, D.F.; Moftah, B.A.; Porter, R.; Wright, D.H. Hyperfine effect in μ^- capture on ^{23}Na and g_p/g_a. *Phys. Rev. Lett.* **1994**, *72*, 3472–3475. https://doi.org/10.1103/PhysRevLett.72.3472.
22. Jonkmans, G.; Ahmad, S.; Armstrong, D.S.; Azuelos, G.; Bertl, W.; Blecher, M.; Chen, C.Q.; Depommier, P.; Doyle, B.C.; von Egidy, T.; et al. Radiative Muon Capture on Hydrogen and the Induced Pseudoscalar Coupling. *Phys. Rev. Lett.* **1996**, *77*, 4512–4515. https://doi.org/10.1103/PhysRevLett.77.4512.
23. Gazit, D. Muon capture on ^{3}He and the weak structure of the nucleon. *Physics Letters B* **2008**, *666*, 472–476. https://doi.org/https://doi.org/10.1016/j.physletb.2008.08.008.
24. Marcucci, L.E.; Kievsky, A.; Rosati, S.; Schiavilla, R.; Viviani, M. Chiral Effective Field Theory Predictions for Muon Capture on Deuteron and ^{3}He. *Phys. Rev. Lett.* **2012**, *108*, 052502. https://doi.org/10.1103/PhysRevLett.108.052502.
25. Brudanin, V.; Egorov, V.; Filipova, T.; Kachalkin, A.; Kovalenko, V.; Salamatin, A.; Shitov, Y.; Štekl, I.; Vassiliev, S.; Vorobel, V.; et al. Measurement of the induced pseudoscalar form factor in the capture of polarized muons by Si nuclei. *Nuclear Physics A* **1995**, *587*, 577–595. https://doi.org/https://doi.org/10.1016/0375-9474(95)00052-3.

26. Siiskonen, T.; Suhonen, J.; Kuz'min, V.; Tetereva, T. Shell-model study of partial muon-capture rates in light nuclei. *Nuclear Physics A* **1998**, *635*, 446–469. https://doi.org/https://doi.org/10.1016/S0375-9474(98)00182-1.
27. Siiskonen, T.; Suhonen, J.; Kuz'min, V.; Tetereva, T. Shell-model study of partial muon-capture rates in light nuclei. *Nuclear Physics A* **1999**, *651*, 437–438. https://doi.org/https://doi.org/10.1016/S0375-9474(99)00153-0.
28. Siiskonen, T.; Suhonen, J.; Hjorth-Jensen, M. Towards the solution of the C_P/C_A anomaly in shell-model calculations of muon capture. *Phys. Rev. C* **1999**, *59*, R1839–R1843. https://doi.org/10.1103/PhysRevC.59.R1839.
29. Gorringe, T.; Fearing, H.W. Induced pseudoscalar coupling of the proton weak interaction. *Rev. Mod. Phys.* **2003**, *76*, 31–91. https://doi.org/10.1103/RevModPhys.76.31.
30. Araujo G.R., Bajpai D., B.L.e.a. The Monument experiment: ordinary muon capture studies for $0\nu\beta\beta$ decay. *Eur. Phys. J. C* **2024**, *84*, 1188. https://doi.org/https://doi.org/10.1140/epjc/s10052-024-13470-6.
31. Jokiniemi, L.; Suhonen, J. Comparative analysis of muon-capture and $0\nu\beta\beta$-decay matrix elements. *Phys. Rev. C* **2020**, *102*, 024303. https://doi.org/10.1103/PhysRevC.102.024303.
32. Gimeno, P.; Jokiniemi, L.; Kotila, J.; Ramalho, M.; Suhonen, J. Ordinary Muon Capture on ^{136}Ba: Comparative Study Using the Shell Model and pnQRPA. *Universe* **2023**, *9*. https://doi.org/10.3390/universe9060270.
33. Suhonen, J. *From Nucleons to Nucleus: Concepts of Microscopic Nuclear Theory*; Springer Berlin, Heidelberg, 2007.
34. Jokiniemi, L.; Suhonen, J.; Ejiri, H.; Hashim, I. Pinning down the strength function for ordinary muon capture on ^{100}Mo. *Physics Letters B* **2019**, *794*, 143–147. https://doi.org/https://doi.org/10.1016/j.physletb.2019.05.037.
35. Jokiniemi, L.; Suhonen, J. Muon-capture strength functions in intermediate nuclei of $0\nu\beta\beta$ decays. *Phys. Rev. C* **2019**, *100*, 014619. https://doi.org/10.1103/PhysRevC.100.014619.
36. Jokiniemi, L.; Miyagi, T.; Stroberg, S.R.; Holt, J.D.; Kotila, J.; Suhonen, J. Ab initio calculation of muon capture on ^{24}Mg. *Phys. Rev. C* **2023**, *107*, 014327. https://doi.org/10.1103/PhysRevC.107.014327.
37. Hyvärinen, J.; Suhonen, J. Nuclear matrix elements for $0\nu\beta\beta$ decays with light or heavy Majorana-neutrino exchange. *Phys. Rev. C* **2015**, *91*, 024613. https://doi.org/10.1103/PhysRevC.91.024613.